ELSEVIER

Polymer 42 (2001) 3503–3514

polymer

www.elsevier.nl/locate/polymer

Morphology and mechanical properties of poly(methylmethacrylate)-*b*-poly(alkylacrylate)-*b*-poly(methylmethacrylate)

J.D. Tong[a], Ph. Leclère[b], C. Doneux[b], J.L. Brédas[b], R. Lazzaroni[b], R. Jérôme[a,*]

[a]*Center for Education and Research on Macromolecules (CERM), University of Liège, Sart-Tilman, B6, B-4000 Liège, Belgium*
[b]*Service de Chimie des Matériaux Nouveaux, Centre de Recherche en Electronique et Photonique Moléculaires, Université de Mons-Hainaut, Place du Parc, 20, B-7000 Mons, Belgium*

Received 8 June 2000; received in revised form 7 September 2000; accepted 16 October 2000

Abstract

A series of well-defined poly(methylmethacrylate) (PMMA)-*b*-poly(alkylacrylate)-*b*-PMMA triblock copolymers (MAM) has been synthesized by transalcoholysis of PMMA-*b*-poly(*tert*-butylacrylate)-*b*-PMMA precursors by alkyl alcohols. The molecular weight (MW) of the outer PMMA blocks is in the 10,000–50,000 range, compared to 50,000–200,000 for the inner poly(alkylacrylate) block. Phase separation, as studied in direct space by atomic force microscopy, is observed for all the investigated triblock copolymers, except for the PMMA-*b*-poly(ethylacrylate)-*b*-PMMA and the PMMA-*b*-poly(*n*-propylacrylate)-*b*-PMMA triblocks of 10,000–50,000–10,000 MW. The ultimate tensile strength measured for the MAM triblocks is strongly dependent on the MW between chain entanglements for the central block. The tensile behavior is however affected by the partial miscibility of the outer and inner blocks when the PMMA MW is low. When this situation prevails, it makes the melt processing possible at temperatures lower than 200°C.

Keywords: Transalcoholysis; Triblock copolymers; Rheological behavior; Atomic force microscopy

1. Introduction

Triblock copolymers consisting of outer polystyrene blocks (PS) and inner rubbery polybutadiene (PB) or polyisoprene (PIP) block (SBS and SIPS) are very well-known thermoplastic elastomers (TPEs). Their unique thermomechanical properties are associated with the dispersion of hard PS microdomains in a continuous rubbery matrix. This physical network of flexible chains combines the mechanical performances of vulcanized rubbers and the straightforward processing of thermoplastics. The use of diene-based TPEs is however limited by the poor oxidation resistance of the unsaturated central block and the relatively low service temperature (60–70°C) controlled by the glass transition temperature of polystyrene. Accordingly, efforts have been made to improve the performances of TPEs by changing either the outer [1–5] or the inner [2,6] blocks. Substitution of fully (meth)acrylate TPEs for the traditional styrene-diene based materials is worth being considered since merely changing the alkyl substituent of the ester group allows a large range of properties to be covered. For instance, the glass transition temperature (T_g) extends from −50°C for poly(isooctylacrylate) up to 190°C for poly(isobornylmethacrylate). Furthermore, immiscibility of alkyl polymethacrylates and polyacrylates is the rule, although some exceptions can be found in the cases of small alkyl groups and low molecular weight (MW) [7]. The much better resistance of poly(meth)acrylates to UV and oxidation compared to polydienes is an additional advantage.

The advent of the ligated anionic polymerization of alkyl (meth)acrylates has allowed for the controlled synthesis of poly(methylmethacrylate) (PMMA)-*b*-poly(*tert*-butylacrylate)-*b*-PMMA triblocks (M*t*BM), which are precursors of a series of PMMA-*b*-poly(alkylacrylate)-*b*-PMMA copolymers (MAM) as result of the selective transalcoholysis of the *tert*-butyl groups of the central block by alkyl alcohols (e.g. 2-ethylhexanol, *n*-butanol) [8]. The mechanical properties of these MAM triblocks are however disappointing, i.e. $\sigma_B < 7.0$ MPa and $\epsilon < 350\%$. McGrath et al. have also observed poor mechanical properties for the poly(methacrylic acid)-*b*-poly(2-ethylhexylmethacrylate)-*b*-poly(methacrylic acid) triblock and the neutralized version [9]. Yasuda et al. have prepared PMMA-*b*-poly(*n*-butylacrylate)-*b*-PMMA (M*n*BM) and PMMA-*b*-poly(ethylacrylate)-*b*-PMMA (MEM) triblocks by rare earth metal

* Corresponding author. Tel.: +32-4-366-3565; fax: +32-4-366-3497.
E-mail address: rjerome@ulg.ac.be (R. Jérôme).

0032-3861/01/$ - see front matter
PII: S0032-3861(00)00759-X

complexes catalyzed living polymerization [10]. Once again, the mechanical properties of these materials are poor compared to SBS, SIPS, and PMMA-poly(butadiene)-PMMA (MBM) triblocks [4,5]. The direct synthesis of MAM triblock copolymers by controlled radical polymerization, e.g. M*n*BM triblocks [11], has not improved significantly this situation ($\sigma_B < 10$ MPa and $\epsilon < 500\%$). Several reasons could account for the poor mechanical properties of these fully (meth)acrylate triblocks, such as (partial) miscibility of the blocks [12], sample preparation by compression molding [8], too short outer blocks [9], and poor control of the block copolymer structure [10,11]. Moreover, the rheological properties of the fully (meth)acrylic triblocks have not been studied in detail, although this issue is of prime importance for the melt processing of these potential TPEs. All what we know is that the average MW between chain entanglements (M_e) for the central block dominates the elastomeric properties, whereas M_e for the outer blocks is thought to have an important effect on the rheological behavior of the MAM triblocks [13].

This paper aims at comparing the morphology, the dynamic mechanical properties, the tensile properties and the flow behavior of MAM triblock copolymers, where the central poly(alkylacrylate) block (A) is, respectively, poly(isooctylacrylate) (MIM series), poly(*n*-butylacrylate) (M*n*BM series), poly(*n*-propylacrylate (M*n*PM series) and poly(ethylacrylate) (MEM series). The morphology of these copolymers has been investigated by atomic force microscopy (AFM), using a procedure designed to image microdomains of different mechanical properties. For this purpose the AFM microscope was operated in the "tapping-mode" and the amplitude and phase of the oscillating tip were recorded simultaneously at each point of the surface, with a lateral resolution of a few nanometers. This technique provided a topographic image and a cartography of the mechanical properties of the sample surface.

Usually, the dependence of the bulk morphology on the composition of block copolymers is analyzed by scattering techniques and transmission electron microscopy (TEM) [14–22]. However, in the case of fully (meth)acrylate block copolymers, the lack of electronic contrast between the poly(methylmethacrylate) and the poly(alkylacrylate) blocks prevents nanometer scale phase-separated morphology from being directly observed by either TEM or small angle X-ray scattering (SAXS). AFM with phase detection imaging thus appears as the unique technique able to observe phase separation in the (meth)acrylic block copolymers under consideration in this study. This capability relies on the difference in modulus of the thermoplastic microdomains of PMMA and the rubbery phases of poly(alkyl acrylate). It must be noted that, in the case of block copolymers with a sufficiently high electronic contrast, the phase morphology observed by AFM (e.g. spheres, cylinders, or lamellae) was quite representative of the bulk morphology [23–25].

2. Experimental part

2.1. Materials

THF and toluene were purified by refluxing over the deep purple sodium–benzophenone complex. Methylmethacrylate (MMA) and *tert*-butylacrylate (*t*BA) (Aldrich) were refluxed over CaH_2, vacuum distilled, and stored under nitrogen at −20°C. Before polymerization, they were added with 10 wt% $AlEt_3$ solution in hexane until a persistent yellowish green color was observed, and distilled under reduced pressure just prior to use (*t*BA was diluted by the same volume of toluene before distillation). *Sec*-Butyllithium (*s*-BuLi) (Aldrich, 1.3 M solution in cyclohexane) was diluted by cyclohexane (ca 0.25 N). 1,1-diphenylethylene (DPE, Aldrich) was vacuum distilled over *s*-BuLi and diluted by toluene (ca. 0.3 N). Isooctyl alcohol, *n*-butanol, *n*-propanol, and ethanol (99%) were used as received. LiCl (99.99%, Aldrich) was dried under vacuum at 130°C.

2.2. Synthesis of the MtBM precursors

A known amount of LiCl was added to a glass reactor that was flamed under vacuum and purged with nitrogen. THF and 1,1-diphenylethylene (DPE) were transferred into the glass reactor through rubbery septa and stainless steel capillaries or syringes. Three-fold molar excess DPE and five-fold molar excess LiCl were used with respect to the initiator (*s*-BuLi). The initiator solution was then added dropwise until a red color persisted, followed by the desired amount of initiator. The solution was cooled down to −78°C and added with the required amount of MMA. The polymerization was conducted at −78°C for 1 h. Upon MMA addition, the deep red color of the initiator immediately disappeared, indicating an instantaneous initiation. The sequential addition and polymerization of *t*BA and MMA were carried out under the same experimental conditions. The copolymerization product was quenched by degassed methanol and the final solution was concentrated before being precipitated into an excess of 90/10 (v/v) methanol/water mixture under stirring. The crude copolymer was dried under vacuum at 60–80°C overnight.

2.3. Preparation of the MAM block copolymers

The best conditions for the transalcoholysis of the *t*BA units of M*t*BM copolymers consisted in dissolving the copolymer in an excess of alkyl alcohol in the presence of *p*-toluenesulfonic acid (PTSA; 10 mol% with respect to the *t*BA units). After reflux at 100–150°C (depending on the boiling point of the alcohols) for 48 h, the copolymer was recovered by precipitation in methanol (in the case of MIM and M*n*BM) or in water (in the case of M*n*PM and MEM) and dried under vacuum at 80°C overnight.

Table 1 lists the MAM triblocks that were synthesized. M_n, M_w/M_n, and composition were determined by size exclusion chromatography (SEC) and NMR.

Table 1
Molecular characteristics of the MAM triblocks analyzed in this study

Sample code	Alkylacrylate	M_n ($\times 10^{-3}$)	M_w/M_n	wt% PMMA
I1	Isooctyl	10–50–10	1.08	28.6
I2	Isooctyl	20–140–20	1.04	22.2
I3	Isooctyl	20–70–20	1.08	36.4
I4	Isooctyl	30–140–30	1.07	30.0
I5	Isooctyl	50–140–50	1.07	41.7
B1	*n*-Butyl	10–50–10	1.08	28.6
B2	*n*-Butyl	15–100–15	1.08	23.1
B3	*n*-Butyl	20–100–20	1.06	28.6
B4	*n*-Butyl	30–150–30	1.05	28.6
B5	*n*-Butyl	30–100–30	1.13	37.5
B6	*n*-Butyl	40–210–40	1.07	27.6
B7	*n*-Butyl	50–100–50	1.05	50.0
P1	*n*-Propyl	10–50–10	1.09	28.6
P2	*n*-Propyl	20–90–20	1.06	30.8
P3	*n*-Propyl	20–150–20	1.05	21.1
P4	*n*-Propyl	40–195–40	1.07	29.1
E1	Ethyl	10–50–10	1.09	28.6
E2	Ethyl	20–80–20	1.06	33.3
E3	Ethyl	20–135–20	1.05	22.8
E4	Ethyl	30–110–30	1.05	35.3
E5	Ethyl	40–170–40	1.07	32

2.4. Sample preparation

For mechanical and rheological measurements, the films were prepared by casting a copolymer solution in toluene (8 wt%; 160 ml) in 100 mm diameter polyethylene dish. The solvent was let to evaporate over 3–4 days at room temperature. The films were dried to constant weight in a vacuum oven at 80°C for 1 day. They were colorless, transparent and elastomeric with a smooth surface. In view of the AFM analysis, dilute solutions of the triblock copolymers in toluene (2 mg/ml) were cast onto mica. The solvent was let to evaporate very slowly for a few days, the system being sheltered from dust anytime. The films were further annealed at 140°C under high vacuum (10^{-7} T) for 24 h. The final film thickness was ca. 500 nm.

2.5. AFM imaging

All the AFM images were recorded with a Nanoscope III microscope from Digital Instruments Inc. operated at room temperature in the Tapping Mode [26] in air. Microfabricated cantilevers with a spring constant of 30 Nm^{-1} were used. The instrument was equipped with the Extender™ Electronics Module to provide simultaneously height and phase cartography. Since the absolute phase contrast strongly depends on the experimental parameters (tip shape, drive amplitude, amplitude set-point), the best contrast was searched for so that the working parameters were not the same for all the samples. Therefore, apparent differences in the phase contrast of the AFM pictures have no reliable meaning here. Images were recorded from different area of each sample, and the time for scanning was ca. 5 min. All the images were collected with the maximum available number of pixels (512) in each direction. For image analysis, the Nanoscope image processing software was used.

2.6. Rheological measurements

The RSI ARES rheometer equipped with a force balance transducer was used, with, either the cone-plate geometry (plate: 25 mm diameter; cone: 4° angle; gap: 56 μm between the cone tip and the plate) for the poly(alkylacrylate)s or the parallel plate geometry (25 mm diameter) for the triblocks. The dynamic storage and loss moduli, G' and G'', were measured as function of angular frequency at various temperatures. The temperature control was better than 1°C. The applied strain was kept within the linear viscoelastic regime, whatever the temperature. The Polymer Laboratory DMTA (parallel plate with 7 mm diameter) was used to conduct temperature sweep experiments at 1 Hz (heating rate: 2°C/min).

2.7. Tensile tests

Mechanical properties were measured with an Adamel Lhomargy tensile tester. Microdumbells were cut from solution cast films and extended at 100 mm/min at room temperature. Strain was measured from the crosshead displacement. Sample thickness and width were 1.5 and 4 mm, respectively. At least three independent measurements were recorded for each sample.

3. Results and discussion

3.1. Structure and morphology

The prerequisite for A–B–A triblock copolymers to be TPEs is that the self-assembly of the copolymer chains leads to the formation of thermoplastic microdomains of A dispersed in the rubbery matrix of B. The formation of this physical network however depends strongly on the phase separation, and thus on the immiscibility of the constitutive blocks A and B. As pointed out in the Introduction, the electronic contrast between the constitutive (meth)acrylic blocks of the copolymers investigated in this study is too low for the nanophase-separated morphology to be directly observed by TEM and SAXS, as is usually the case. Therefore, the best strategy is to analyze the phase morphology by combining AFM and dynamic mechanical analysis (DMA). In the case of PMMA–poly(alkylacrylate)–PMMA copolymers, the immiscibility can be estimated from the polymer–polymer interaction parameter, χ [27], for the PMMA/poly(alkylacrylate) pair.

It is predicted to decrease as the alkyl group is changed in the order of isooctyl > *n*-butyl > *n*-propyl or ethyl [28], so that the miscibility of PMMA with the poly(alkylacrylates) should increase in the same direction. Previous observations have shown that the phase separation of the PMMA–PIOA–

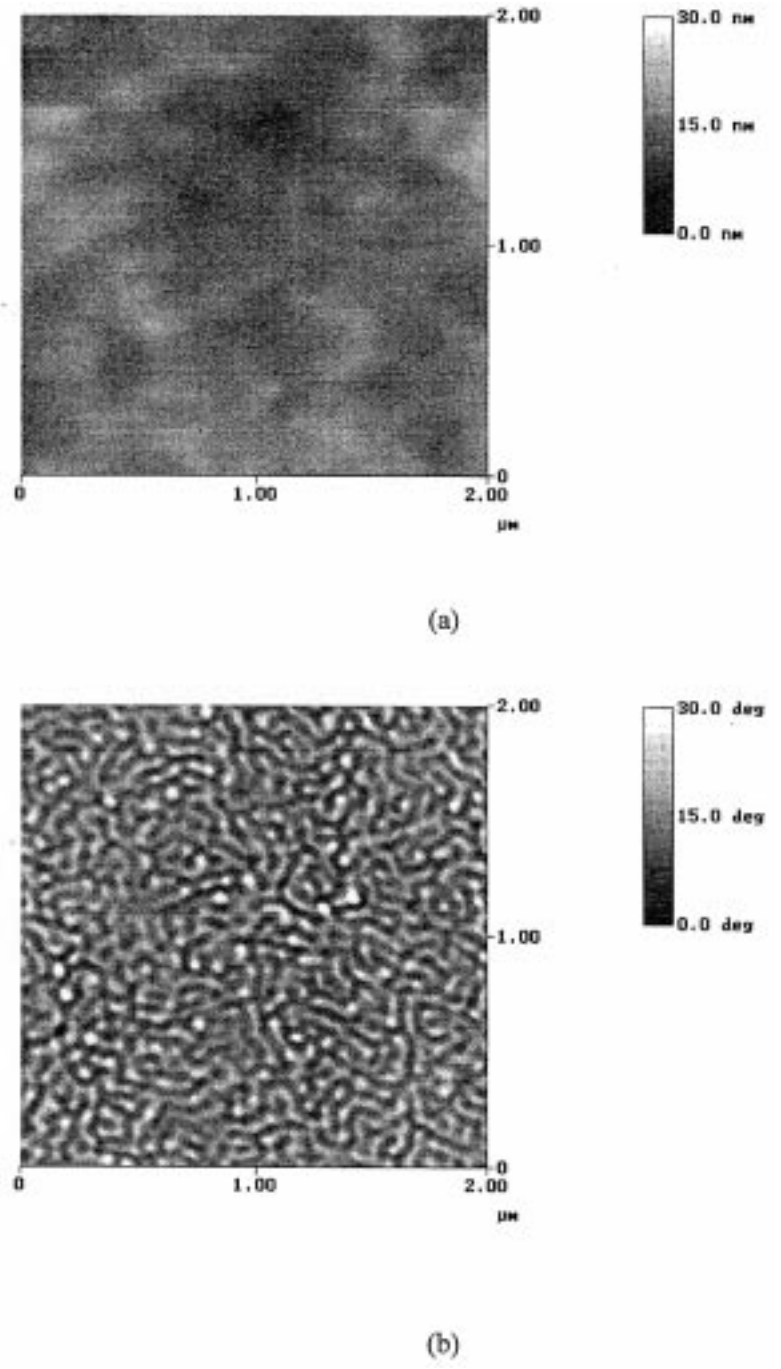

Fig. 1. $2 \times 2\ \mu m^2$ tapping-mode AFM images: topographic (a; vertical grayscale: 30 nm) and phase (b) images of MIM sample I5; phase images of M*n*BM sample B4 (c), M*n*PM sample P3 (d), MEM sample E3 (e), and M*n*PM sample P1 (f).

PMMA triblocks (MIM) is sharp (e.g. T_g of PIOA is independent of the PMMA content and MW), to the point where the "sphere in a matrix" morphology is observed with AFM even when PMMA MW is as low as 3500 (PIOA MW:100,000) [13].

It has been recently shown that the phase of the oscillating cantilever in tapping-mode AFM strongly depends on the tip-sample interaction so that it can be used to discriminate constitutive components of multiphase polymeric materials [29–31]. Indeed, when the amplitude of the oscillation is only slightly reduced (i.e. by less than 20%) upon contact with the surface, the phase of the cantilever can then be related to the elastic modulus of the probed area [32]. Therefore, the observation of at least two regions with different phase signals on the AFM images of block copolymers is clear indication of microphase separation.

Fig. 1 shows a series of AFM images observed for triblock copolymers listed in Table 1. It must be noted

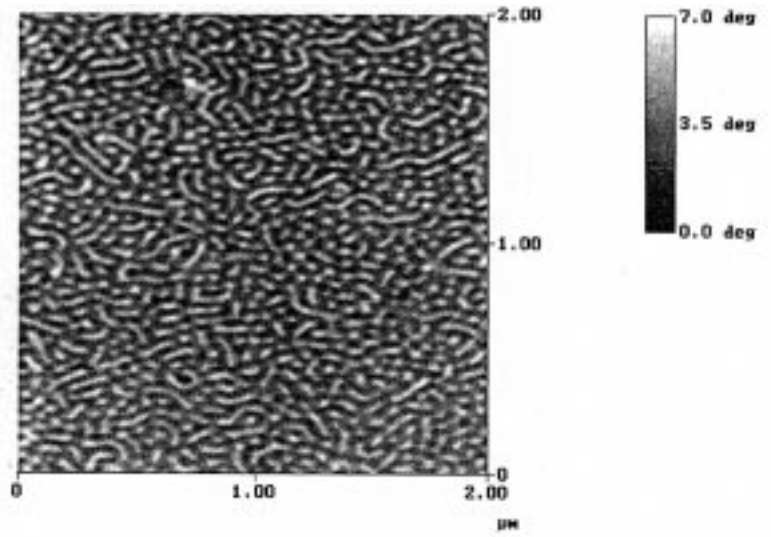

(c)

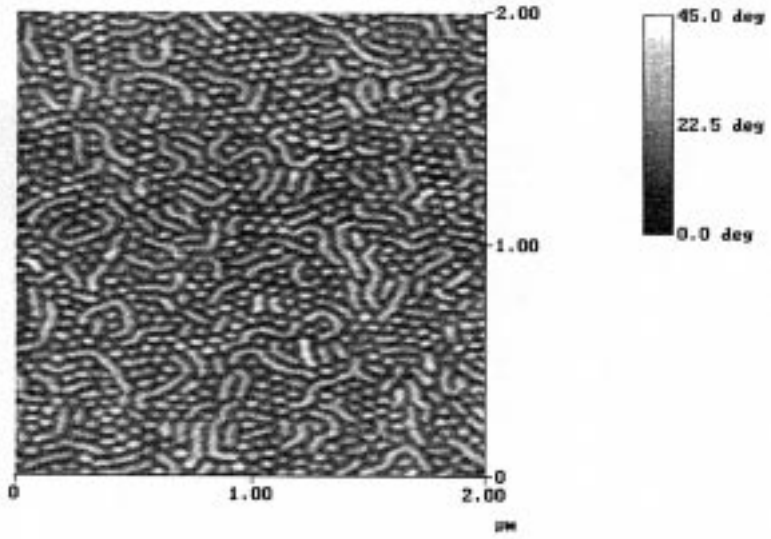

(d)

Fig. 1. (*continued*)

that either cylindrical or lamellar phase morphology should be predicted for all these copolymers on the basis of their composition. As a rule, the topographic images are almost featureless, which indicates that the film surface is smooth (over 2×2 μm^2 area, the roughness does not exceed a few nanometers). A typical example is shown in Fig. 1a for the MIM sample I5. In sharp contrast, the phase image for the same sample (Fig. 1b) is highly textured, consisting of a complex pattern of bright and dark elongated objects. This pattern is interpreted as the interpenetrated assembly of PMMA and PIA lamellae, consistently with the aforementioned copolymer composition. As previously explained, the brighter areas that correspond to larger phase values, are typical of component of higher modulus, i.e. PMMA, whereas the darker areas are the signature of the softer component (polyisooctylacrylate in this case). It must

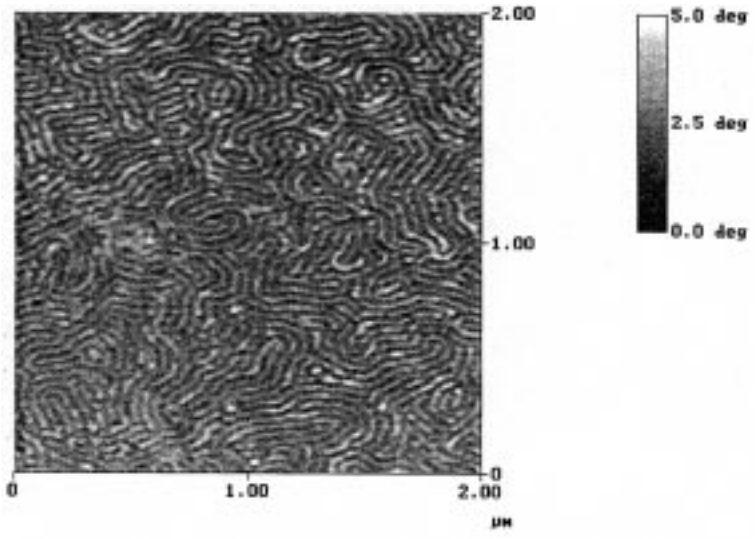

(e)

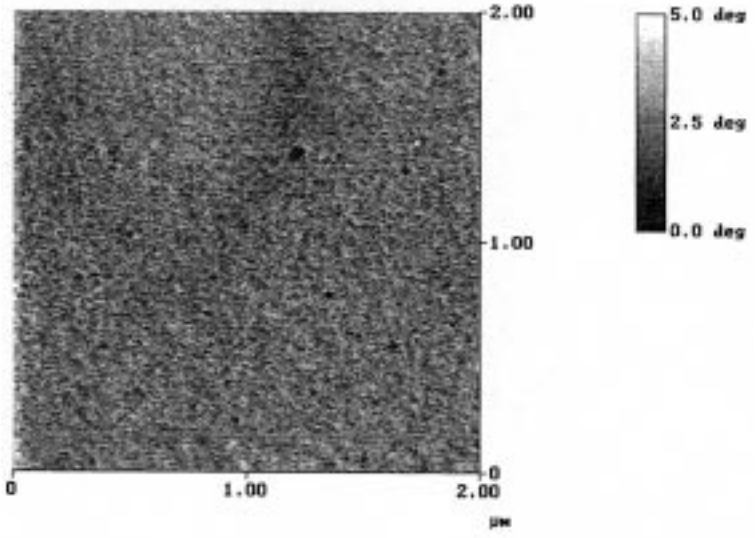

(f)

Fig. 1. (*continued*)

also be noted that the phase image is not reminiscent at all of the topographic profile. It is fully dominated by the local contrast in the mechanical properties, being accordingly clear evidence for microphase separation in this bulk triblock copolymer.

The systematic AFM analysis of the samples listed in Table 1 has confirmed, in most the cases, a microdomain morphology consistently with the expectation based on the copolymer composition [33]. For instance, Fig. 1c shows the morphology for the 30,000–150,000–30,000 M*n*BM copolymer (sample B4). Bright dots and bright elongated objects coexist in a darker continuous matrix. This observation is thought to originate from PMMA cylinders (bright areas), within the poly(*n*-butylacrylate) matrix either standing perpendicular or lying parallel to the surface. That the diameter of the dots is identical to the width of the flat cylinders ($19 + /-1$ nm) is in line with this hypothesis. As explained in a previous paper [34], the most stable

arrangement of the PMMA cylinders is perpendicular to the surface, in agreement with the higher surface energy of PMMA compared to poly(alkylacrylate) [28]. The system tends indeed to organize itself so as to minimize the amount of PMMA at the surface, thus by exposing only the apex of the PMMA cylinders. In Fig. 1c, the sample has more likely not reached the thermodynamic equilibrium, since flat cylinders are still visible on the surface and the ratio of standing/flat cylinders tends to increase upon annealing. A similar situation is shown by Fig. 1d for the 20,000–150,000–20,000 M*n*PM copolymer (sample P3). However, the standing cylinders outnumber the flat counterparts and the perpendicular cylinders locally appear to self-organize according to a hexagonal-close-packed lattice, as theoretically predicted [33] and observed in the bulk of other block copolymers [14–22]. It must be reminded that the phase morphology of the block copolymers under consideration cannot be analyzed by the "classical" techniques of TEM and small-angle X-ray scattering, because of the very small contrast in the electron density of the constituents and the lack of selective staining agents. AFM is thus the best if not the only method which can be dedicated to the analysis of the morphology of fully (meth)acrylate block copolymers.

The image of Fig. 1e is characteristic of the MEM sample E3 (20,000–135,000–20,000). The AFM picture clearly shows a lamellar morphology. The hypothesis of assembly of cylinders all lying flat on the surface is not reasonable, since the morphology remains unchanged upon extended annealing. Moreover, according to our experience, "bifurcations" ("three-way crossroads" as observed in this picture) are only observed in lamellar organization and not in assemblies of flat cylinders (see Fig. 1c and d). The formation of alternating PMMA and PEA lamellae in sample E3 is somehow surprising, for a highly asymmetric composition. The PMMA/PEA wt. ratio of ca. 23:77 is indeed expected to generate a cylindrical morphology. This apparent contradiction is under current investigation.

The major conclusion from Fig. 1e is that microphase separation can actually occur, even when the chemical structure of the blocks is very similar (MMA and ethylacrylate are isomers). However, for lower MWs (samples E1 and E2), the AFM phase images are completely featureless, indicating the absence of microphase separation. This is also the case for the 10,000–50,000–10,000 M*n*PM copolymer (sample P1; Fig. 1f), whereas the MIM and M*n*BM copolymers all show microphase separation, independently of their MW. This observation is consistent with the increasing misciblity of blocks of more similar structure (i.e. when the alkyl group gets shorter) and lower MW. Based on the AFM observations, samples E1, E2, and P1 should not typically behave as TPE's, in contrast to all the other copolymers analyzed in this study.

The main conclusions about the miscibility of the poly(meth)acrylate blocks based on AFM have been confirmed by DMA. For instance, Fig. 2 shows that T_g (at maximum tan δ) for PMMA increases (from 116 to 138°C) and T_g of

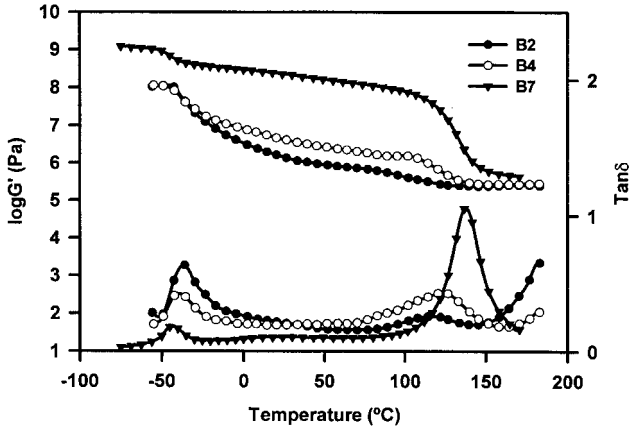

Fig. 2. Temperature dependence of tan δ and G' for the B2, B3 and B7 samples of the M*n*BM series (Table 1).

P*n*BA decreases (from −38 to −42°C) when the content (and thus MW) of PMMA is increased in the M*n*BM series (samples B2, B3, B7). This observation is consistent with some partial miscibility of PMMA and P*n*BA, which decreases when the length of PMMA is increased, the MW of P*n*BA being kept unchanged. Fig. 3 compares the temperature dependence of tan δ for two M*n*PM samples (P1 and P3; Table 1). When the PMMA MW is 20,000 (sample P3), two T_gs are observed at −25°C (for the P*n*PA block) and at 110°C (for the PMMA blocks), which is the signature of a phase-separated structure. The PMMA glass transition peak is however rather broad (broader compared to the parent MIM and M*n*BM triblocks), which more likely indicates some miscibility of the two blocks. A decrease of the PMMA MW from 20,000 to 10,000 (sample

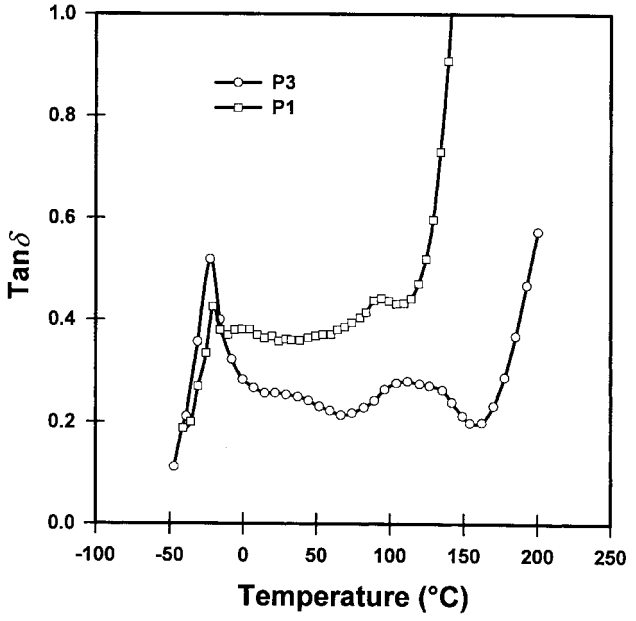

Fig. 3. Temperature dependence of tan δ for the P1 and P3 samples of the M*n*PM series (Table 1).

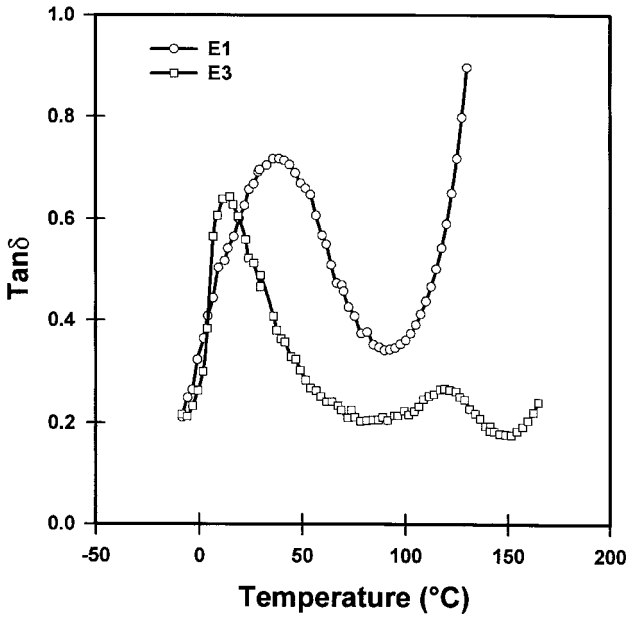

Fig. 4. Temperature dependence of tan δ for the E1 and E3 samples of the MEM series (Table 1).

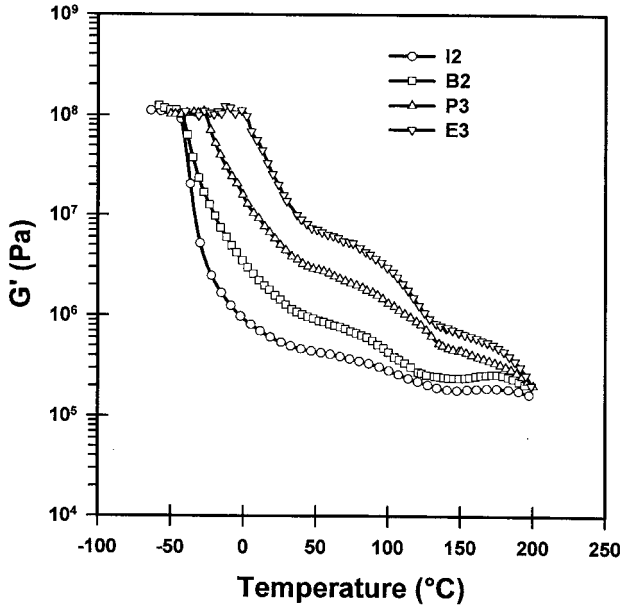

Fig. 5. Temperature dependence of storage modulus, G', for the I2, B2, P3 and E3 samples (Table 1). The PMMA wt% is ca. 22–23% for each sample.

P1) results in a quasi-continuous transition from ca. −20 to 90°C, which emphasizes a high degree of miscibility of the PMMA and the P*n*PA blocks. This increase in miscibility facilitates the relaxation of the individual copolymer chains [35–37], keeping tan δ high in a large temperature range. Fig. 4 is a comparison of the tan δ–temperature curves for two MEM samples (E1 and E3; Table 1) of molecular structure quite comparable to the M*n*PM samples analyzed in Fig. 3. Although the E3 sample (PMMA block of 20,000 MW) shows essentially the same curve as the M*n*BM (B3) and M*n*PM (P3) analogues, i.e. two separate T_gs characteristic of the hard PMMA block and the soft poly(alkylacrylate) block, respectively, only one very broad transition (−10 to 90°C) with a maximum at ca. 40°C is observed when the PMMA length is decreased by a factor of two (E1 sample). Thus, within the detection limits of DMTA, no phase separation is detected when two short-length PMMA blocks (10,000 MW) are combined with poly(ethylacrylate) (50,000 MW; sample E1, in Fig. 4) in contrast to what happens when the central block is poly(*n*-propylacrylate) (sample P1, in Fig. 3), a partial miscibility being then observed. These conclusions are in qualitative agreement with the AFM observations. When the central block of the MAM triblocks is changed, not only the miscibility of the two blocks is modified, but also T_g of the rubbery block and the modulus of the rubbery plateau. Fig. 5 compares the temperature dependence of the storage modulus for a series of MAM triblocks (I2, B2, P3, and E3; Table 1) of quite similar composition (ca. 22–23 wt% PMMA) and phase morphology. Expectedly, G' at the end of the glassy plateau decreases from −40°C for the MIM and M*n*BM triblocks, to −25°C and 5°C for the M*n*PM, and MEM triblocks, respectively. The most important difference has to be found in the modulus of the rubbery plateau, which increases when the size of the alkyl ester group of the midblock is decreased (from isooctyl to ethyl), thus with the average MW between the chain entanglements of this block.

3.2. Tensile properties

According to reports on PS-*b*-B-*b*-PS (SBS) and PS-*b*-PIP-*b*-PS (SIPS) triblock copolymers, the ultimate tensile strength and elongation at break are as high as 30 MPa and 800%, respectively [38]. The high performances of these materials compared to the unreinforced vulcanizates of SBR rubbers are explained by the reinforcement of the rubber by the hard polystyrene microdomains and by the slippage of the entangled rubbery chains which contributes to delay the ductile failure of the PS microdomains [38–40]. We have previously reported that the mechanical properties of MIM and M*n*BM triblocks are usually poor when compared to the traditional diene-based TPEs [13]. This disappointing observation was tentatively explained by the partial miscibility of the PMMA and PIOA (P*n*BA) blocks particularly when the PMMA MW and content are low (i.e. 20 K, 10%). The most reasonable explanation was however found in the average MW between chain entanglements, M_e, which is much higher for poly(alkylacrylates) than for polydienes. This explanation found support in the initial tensile behavior of MIM triblock (7000–100,000–7000) which is properly accounted for by the classical theory of rubber elasticity [41] and not by the "rubber + filler" model [42], which actually fits the behavior of the styrene-diene TPEs [38]. It must be concluded that the PIOA central blocks

Table 2
Average MW between chain entanglements (M_e) for a series of polymers

Polymer	M_e
Polybutadiene [38]	1700
Polyisoprene [38]	6100
Poly(ethylacrylate)	11,000
Poly(*n*-propylacrylate)	16,000
Poly(*n*-butylacrylate)	28,000
Poly(isooctylacrylate)	59,000

of MIM triblocks are essentially not entangled and that the ultimate tensile strength of MAM triblocks should increase as the length of the alkyl group of the polyacrylate mid-block is decreased, since M_e is then decreasing (Table 2). M_e for the poly(alkylacrylate)s has actually been calculated from Eq. (3) [43–46]:

$$M_e = \rho RT/G_N^0 \quad (3)$$

where $G_N^0 = G'$ (tan $\delta \rightarrow$ min) is the shear modulus in the plateau region, ρ the polymer density, R the gas constant and T the temperature.

In addition to M_e for the poly(alkylacrylate)s, Table 2 also lists M_e for PB and PIP. Table 3 reports the mechanical properties for the four series of MAM triblocks. The highest ultimate tensile strength for each series (i.e. ca. 12 MPa for MIM; 16 MPa for M*n*BM; 17.5 MPa for M*n*PM; and 24 MPa for MEM) actually increases inversely proportional to M_e for the poly(alkylacrylate) mid-block. These data confim the key role of M_e of the mid-rubbery block in the control of the ultimate mechanical properties of triblock type TPEs. Although substitution of poly(ethylacrylate) for poly (isooctylacrylate) results in improved mechanical performances (comparison of e.g. E5 and I5 samples in Table 3), the performances of the triblocks of the MEM series are far from being as good as the classical SIPS of comparable composition. Fig. 6 shows the stress–strain curve characteristic of each series of MAM triblocks, (comparable PMMA MW (15–20,000) and content (22%)), and Fig. 7 is typical of SIPS containing 20 wt% PS [40]. The very well-defined and extended rubbery plateau (Fig. 7) exhibited by the SIPS copolymer ($M_e = 6100$ and $T_g = -70$°C for PIP) is no longer observed for copolymers of the MAM series (Fig. 6). From that point of view, the copolymer E3 of the MEM series is apparently the worst (Fig. 6). In fact, Fig. 5 shows that E3 is at the end of the glass transition and not yet in the rubbery plateau at 25°C. A decrease in the MW of the PMMA block (from 20,000 to 10,000) is enough to restore a situation closer to the expected one when the effect of the mid-poly(alkylacrylate) block is considered (Fig. 8). It is thus clear that no poly(alkylacrylate) is valuable alternative for PIP, because of inappropriate balance of M_e and T_g. Indeed, the desirable decrease of M_e results in higher T_g in the poly (alkylacrylate) series.

3.3. Rheological properties

We have previously reported that MIM and M*n*BM triblocks behave as "vulcanized" elastomers rather than as thermoplastic elastomers beyond T_g of the PMMA microdomains [34], except if the PMMA MW is as low as 5000 for MIM and 8000 for M*n*BM. This is an additional difference with the traditional SBS and SIPS TPEs of comparable molecular structure [47]. Fig. 9a shows, as an example, the typical non-Newtonian behavior of the I1 sample in the

Table 3
Mechanical properties of MAM triblock copolymers

Sample code	Ultimate tensile strength (MPa)	Elongation at break (%)	Initial modulus (MPa)
I1	6.5	320	5
I2	7.1	480	2
I3	11.5	350	96
I4	11.9	440	42
I5	11.8	285	91
B1	12.5	540	15
B2	12.3	720	7
B3	14.7	610	31
B4	15.0	700	25
B5	15.2	380	180
B6	15.2	700	26
B7	16.1	230	570
P1	14.0	660	23
P2	14.5	600	11
P3	15.2	680	9
P4	17.5	650	30
E1	9.6	540	12
E2	18.5	350	79
E3	16.4	390	26
E4	23.2	280	181
E5	23.8	350	160

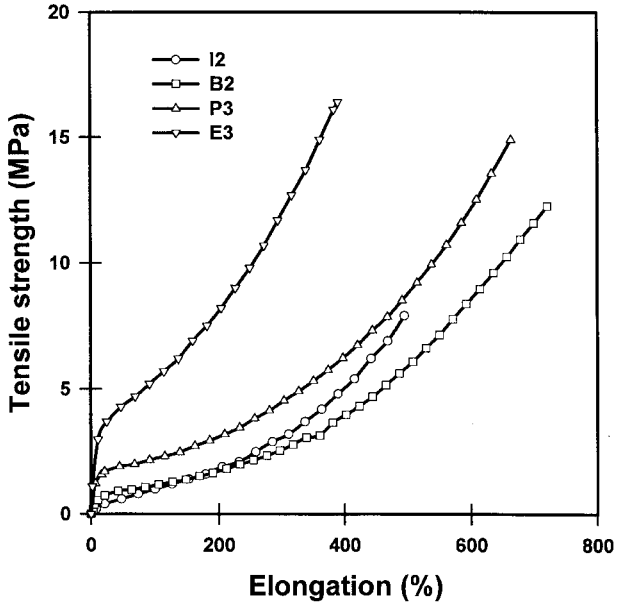

Fig. 6. Tensile curves for the I2, B2, P3 and E3 samples, that contain ca. 22–23 wt% PMMA.

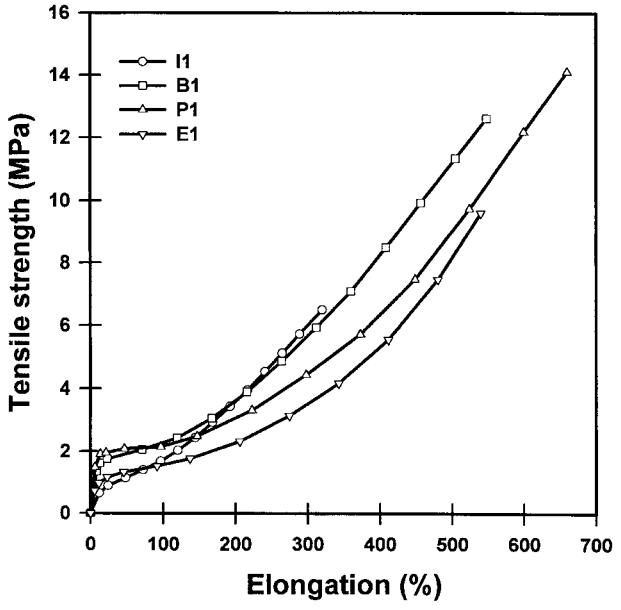

Fig. 8. Tensile curves for the I1, B1, P1 and E1 samples of the same molecular structure (10,000–50,000–10,000).

150–200°C temperature range, thus well beyond T_g of PMMA. This behavior indicates that the domain (ordered) structure of the MIM triblock persists at these high temperatures. This ordered structure is however transformed into disordered (homogeneous) structure when the temperature exceeds a critical value, known as the order–disorder transition temperature (T_{ODT}) [48–52]. At or at least near T_{ODT}, there is transition from non-Newtonian behavior to Newtonian flow. Fig. 9 compares the frequency dependence of the complex viscosity at different temperatures for a series of MAM (I1, B1, P1, and E1 of the same molecular structure). Although the typical non-Newtonian behavior is observed for MIM in the whole frequency and temperature ranges investigated in this study, the situation considerably changes when the PIOA block is replaced by P*n*BA (Fig. 9b), P*n*PA (Fig. 9c) and PEA (Fig. 9d), respectively. For instance, the flow is Newtonian at 190°C (from 1 to 10 Hz) for the P1 and E1 samples in sharp contrast to the B1 and I1 analogues which are typically non-Newtonian.

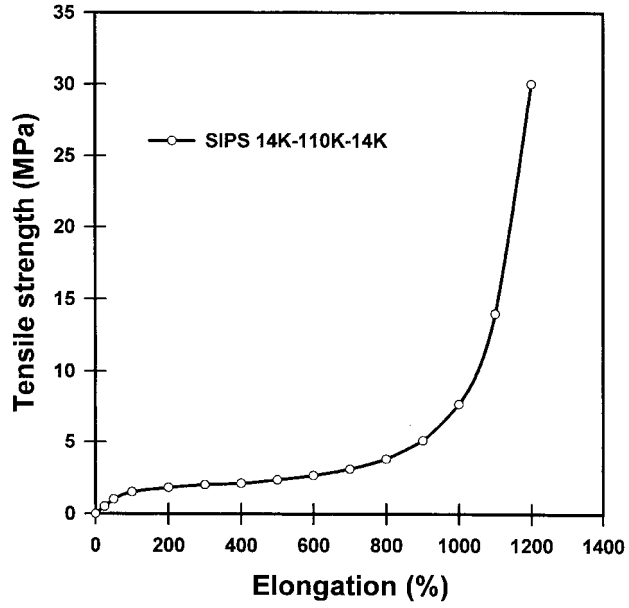

Fig. 7. Tensile curve for the SIPS triblock of 14,000–112,000–14,000.

Bates et al. [53] and Han et al. [54] have recently shown that rheological data can be used to determine the order–disorder transition temperature of block copolymers. Although the methods proposed by these authors differ to some extent, the basic idea is that the rheological properties of the block copolymer must change dramatically at T_{ODT}. Table 4 lists the T_{ODT} determined by the Han's method for comparable MAM triblocks (examples of determination were reported elsewhere [13]). This transition occurs at 170°C in the case of central poly(alkyl acrylate) block with short alkyl substituents (ethyl and *n*-propyl), although it exceeds 200°C for longer alkyl groups (*n*-butyl and iso-octyl). So, as the degree of miscibility of PMMA with poly(alkylacrylate)s increases (see Figs. 2–4 and related comments), the stability of the two-phase structure in the melt decreases and so does T_{ODT}.

4. Conclusions

A series of poly(methylmethacrylate) (MMA)-*b*-poly(alkylacrylate)-*b*-PMMA triblock copolymers (MAM) has been prepared by selective transalcoholysis of the central block of PMMA-*b*-poly(*tert*-butylacrylate) (P*t*BA)-*b*-PMMA precursors by alkyl alcohols. Solution cast films

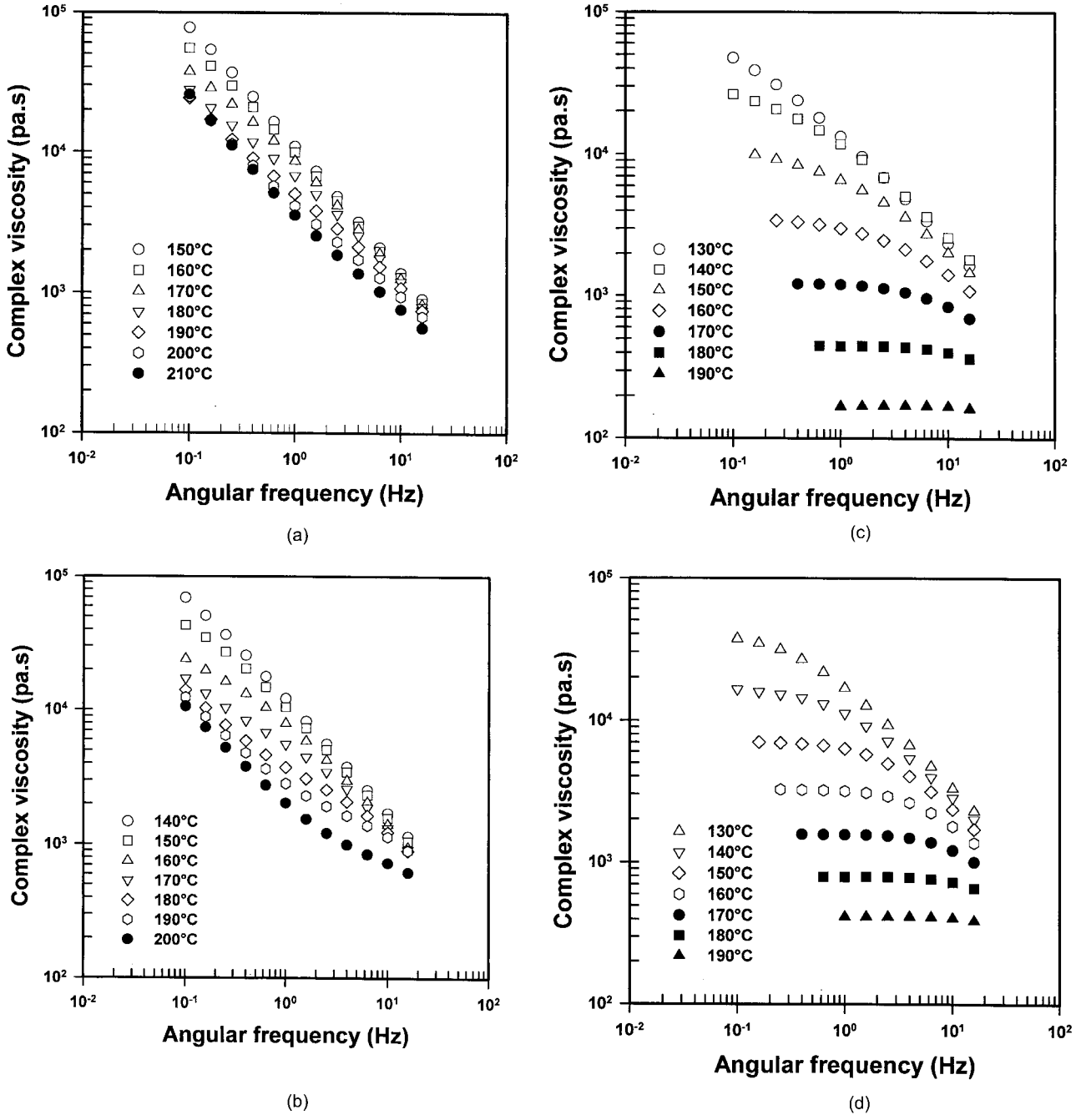

Fig. 9. Plots of complex viscosity vs. angular frequency at different temperatures for: (a) I1; (b) B1; (c) P1 and (d) E1 (Table 1).

Table 4
T_{ODT} of MAM of the same MW and composition (Table 1)

MAM	T_{ODT} (°C)
I1	> 200
B1	> 200
P1	170
E1	170

of MAM triblocks have been characterized by AFM, dynamic and static mechanical analysis. Although phase separation is complete for all the investigated MIM and M*n*BM copolymers, it is adversely influenced by the partial miscibility of the constitutive blocks in the case of M*n*PM and MEM copolymers. For instance, the low MW MEM sample (10,000–50,000–10,000) shows only one intermediate T_g. In case of complete phase separation (PMMA MW higher than 20,000), the ultimate tensile strength of MAM triblocks is found to increase as the size of the alkyl ester

group is decreased. The M_e for the central block is at the origin of this behavior. Whatever the central poly(alkylacrylate) block, the mechanical performances of the MAM triblocks are lower than those ones of traditional SIPS thermoplastic elastomers. The reason is that although M_e and T_g of the central block should be as low as possible, these two parameters are changed in the opposite direction when the alkyl substituent of poly(alkylacrylate)s is changed. The rheological behavior, and thus the processing conditions, are influenced by the partial miscibility of the two blocks of the MAM triblocks. If the immiscibility is complete (MIM and M*n*BM), the triblocks behave as "vulcanized" elastomers, the complex viscosity remaining non-newtonian far above T_g of the hard microdomains. The order–disorder transition is then higher than 200°C. It however decreases down to 170°C when the PEA and P*n*PA mid-blocks show some partial miscibility with PMMA.

Acknowledgements

The authors are grateful to the "Service Fédéraux des Affaires Scientifiques, Techniques et Culturelles" for general support under the auspices of the "PAI 4/11: Supramolecular Chemistry and Supramolecular Catalysis." RL is "Maître de Recherche" by the "Fonds National de la Recherche Scientifique" (FNRS; Belgium).

References

[1] Fetters LJ, Morton M. Macromolecules 1969;2(5):453.
[2] Morton M. In: Legge NR, Holden G, Schroeder HE, editors. Thermoplastic elastomers. Munich: Hanser, 1987 (p. 67).
[3] Morton M, Mikesell SL. J Macromol Sci, Chem 1993;A7(7):1391.
[4] Yu Y, Dubois Ph, Jerôme R, Teyssié Ph. Macromolecules 1996;29:1753 (see also p. 2738).
[5] Yu JM, Dubois Ph, Teyssié Ph, Jerôme R. Macromolecules 1996;29:6090.
[6] Jérôme R, Fayt R, Teyssié Ph. In: Legge NR, Holden G, Schroeder HE, editors. Thermoplastic elastomers, Munich: Hanser, 1987 (p. 451).
[7] Cowie JMG, Ferguson R, Fernandez MD, Fernandez MJ, McEwen IJ. Macromolecules 1992;25:3170.
[8] Jérôme R, Fayt R, Teyssié Ph. In: Legge NR, Holden G, Schroeder HE, editors. Thermoplastic elastomers, vol. 2. Munich: Hanser, 1996 (p. 521).
[9] Venkateshwaran LN, York GA, Deporter CD, McGrath JE, Wilkes GL. Polymers 1992;33:2277.
[10] Ihara E, Morimoto M, Yasuda H. Macromolecules 1995;28:7886.
[11] Tong JD, Moineau G, Leclère Ph, Brédas JL, Lazzeromi R, Jérôme R. Macromolecules 2000;33:470.
[12] Soltani R, Laupretre F, Monnerie L, Teyssie Ph. Polymer 1998;39:3297.
[13] Tong JD, Jérôme R. Polymer 2000;41:2499.
[14] Gallot BRM. Adv Polym Sci 1978;29:85.
[15] Gallot B. In: Blumstein A, editor. Liquid crystalline order in polymers. Academic Press: New York, 1978 (p. 223).
[16] Hashimoto T, Nagatoshi K, Todo A, Hasegawa H, Kawai H. Macromolecules 1974;7:364.
[17] Hashimoto T, Todo A, Itoi H, Kawai H. Macromolecules 1977;10:377.
[18] Todo A, Kiuno H, Miyoshi K, Hashimoto T, Kawai H. Polym Engng Sci 1977;17:587.
[19] Hashimoto T, Shibayama M, Kawai H. Macromolecules 1980;13:1237.
[20] Hashimoto T, Fujimura M, Kawai H. Macromolecules 1980;13:1660.
[21] Thomas EL, Anderson DM, Henkee CS, Hoffman D. Nature 1988;334:598.
[22] Riess G, Bahhadur P. In: Mark HF, Bikales NM, Overberger CG, Menges G, editors. Encyclopedia of polymer science and engineering. New York: Wiley, 1989 (p. 324).
[23] Rasmont A, Leclère Ph, Doneux C, Lambin G, Tong JD, Jérôme R, Brédas JL, Lazzaroni R. Colloids Surf B: Biointerfaces 2001; 13:381.
[24] Leclère Ph, Moineau G, Minet M, Dubois Ph, Jérôme R, Brédas JL, Lazzaroni R. Langmuir 1999;15:3915.
[25] Leclère Ph, Lazzaroni R, Brédas JL, Yu JM, Dubois Ph, Jérôme R. Langmuir 1996;12:4317.
[26] Maganov SN, Whangbo MH, editors. Surface analysis with STM and AFM: experimental and theoretical aspects of image analysis. Weinheim: VCH, 1996 (p. 39).
[27] Fedos RF. J Polym Sci 1969;Pt. C 26:189.
[28] Van Krevelen DW. Properties of polymers, vol. 3. Amsterdam: Elsevier, 1990 (p. 790).
[29] Brandsch R, Bar G, Whangbo MH. Langmuir 1997;13:6349.
[30] Bar G, Brandsch R, Whangbo MH. Langmuir 1997;14:7343.
[31] Cleveland JP, Anczykowski B, Schmidt AE, Elings VB. Appl Phys Lett 1998;72:2613.
[32] Magonov SN, Elings V, Whangbo WH. Surf Sci Lett 1997;375:L385.
[33] Bates FS, Fredrickson GH. Annu Rev Phys Chem 1990;41:525.
[34] Tong JD, Leclère R, Jérôme R et al. Submitted for publication.
[35] Hashimoto T, Tsukahara Y, Tachi K, Kawai H. Macromolecules 1983;16:648.
[36] Kraus G, Rollmann KW. J Polym Sci, Polym Phys Ed 1976;14:1133.
[37] Berglund CA, Mckay KW. Polym Enngg Sci 1993;33:1195.
[38] Holden G, Legge NR. In: Holden G, Legge NR, Quirk R, Schroeder HE, editors. Thermoplastic elastomers, vol. 2. Munich: Hanser, 1996 (p. 47).
[39] Holden G, Bishop ET, Legge NR. J Polym Sci 1969;Pt. C V26:37.
[40] Quirk PR, Morton M. In: Holden G, Legge NR, Quirk R, Schroeder HE, editors. Thermoplastic elastomers, vol. 2. Munich: Hanser, 1996 (p. 71).
[41] Gumbrell SM, Mullins L, Rivlin RS. Trans Faraday Soc 1953;49:1495.
[42] Guth E. J Appl Phys 1945;16:20.
[43] Ferry JD. Viscoelastic properties of polymers, vol. 3. New York: Wiley, 1980.
[44] Graessley WW. Adv Polym Sci 1974;16:58.
[45] Xu Z, Hadjichristidis N, Fetters LJ, Mays JW. Adv Polym Sci 1995;120:1.
[46] Onogi S, Masuda T, Kitagawa K. Macromolecules 1970;3:109.
[47] Han CD, Baek DM, Kim JK, Chu SG. Polymer 1992;33:294.
[48] Helfand E, Wasserman ZR. Macromolecules 1976;9:879.
[49] Leibler L. Macromolecules 1980;13:1062.
[50] Bates FS, Fredrickson GH. In: Holden G, Legge NR, Quirk R, Schroeder HE, editors. Thermoplastic elastomers, vol. 2. Munich: Hanser, 1996 (p. 335).
[51] Hashimoto T. In: Holden G, Legge NR, Quirk R, Schroeder HE, editors. Thermoplastic elastomers, vol. 2. Munich: Hanser, 1996 (p. 429).
[52] Han CD, Baek DM, Kim JK, Ogawa T, Sakamoto N, Hashimoto T. Macromolecules 1995;28:5043.
[53] Rosesale JH, Bates FS. Macromolecules 1990;23:2329.
[54] Han CD, Kim J. J Polym Sci, Part B 1987;25:1741.